

Direct measurement of spectral momentum densities of ordered and disordered semiconductors by high energy EMS

C. Bowles, M.R. Went, A.S. Kheifets and M. Vos

Atomic and Molecular Physics Laboratories, Research School of Physical Sciences and Engineering, Australian National University, Canberra ACT 0200, Australia

Abstract. High Energy solid state electron momentum spectroscopy (EMS) is capable of directly measuring spectral functions of ordered and disordered solid matter. In this paper we investigate the spectral functions for the group IV semiconductors Ge and Si. We attempt to resolve the electronic structure differences in amorphous, polycrystalline and crystalline atomic arrangements of the semiconductors. We examine the experimental differences in polycrystalline and amorphous Ge, and draw conclusions as to the similarities/differences between the two states of matter.

Keywords: Electron Momentum Spectroscopy, band structure, semiconductor, electronic structure
PACS: 61.43.Dq, 71.20.Mq, 71.23.Cq, 73.61.Cw

1. INTRODUCTION

Semiconductor samples can be prepared in an amorphous, polycrystalline or single-crystal form. Each form is expected to have a different electronic structure resulting from differences in the degree of short and long range order. In this paper we will present experimental spectral functions for these three states of order for semiconductors. Single crystals have both short and long range order. Polycrystalline samples consists of many small randomly oriented single crystals separated by grain boundaries. Except for the small number on atoms that are located at the grain boundaries each atom is in a very similar environment as in a single crystal. The measured electronic structure of polycrystalline samples is thus expected to resemble the spherically-averaged electronic structure of a single crystal. Amorphous semiconductors can be described by a continuous random network (CRN) [1]: each atom still has a co-ordination number of four but is positioned in a distorted tetrahedron with a distribution of bond lengths and bond angles. CRN structures are more ordered than a classic amorphous solid. With limited short range order in the CRN samples the question arises, how different is the polycrystalline and amorphous electronic structures of semiconductors?

From a theoretical point of view the amorphous phase presents a challenge as the electronic structure can not be described by Bloch functions due to the absence of a periodicity in the potential. One approach is to approximate the amorphous phase as a crystal with an extremely large, disordered, unit cell [2], another approach is based on Green's function techniques [3]. We will present experimentally measured spectral functions to try to resolve the validity of some of the theoretical assumptions.

In EMS a high energy electron impinges upon a solid target, scattering from a bound electron which is ejected. These two electrons are then measured in coincidence and via

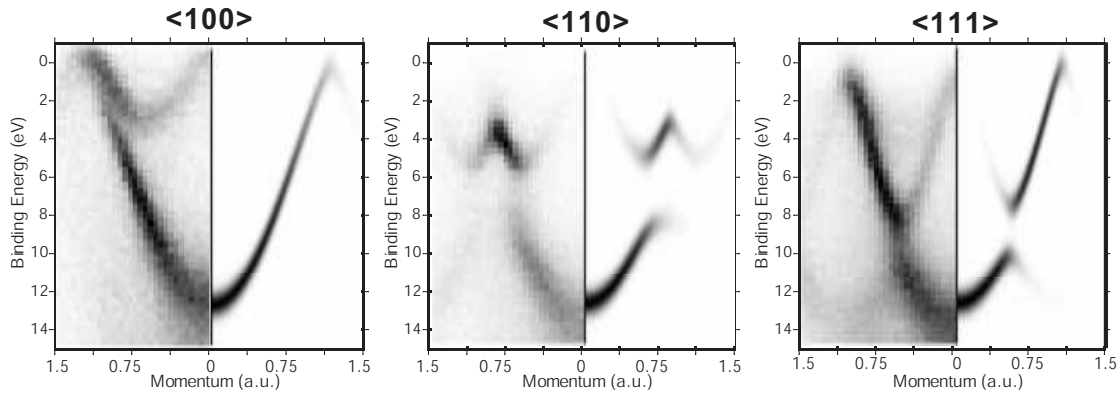


FIGURE 1. The spectral functions for a single crystal silicon sample measured for momenta along the a) $\langle 100 \rangle$, b) $\langle 110 \rangle$, c) $\langle 111 \rangle$ crystallographic direction. Experimental results are shown in the left half, theoretical calculations in the right half of each panel.

conservation laws we can directly determine the binding energy and the momentum of the bound electron an instant before the collision took place [4]. The EMS cross-section can be shown to be directly proportional to the target spectral function, ie the modulus squared of the momentum space one electron wavefunction [5]. In our spectrometer the detectors are positioned in such a way that only target electrons with momentum along the vertical direction contribute to the coincidence count rate. Thus for single crystal targets the anisotropy in the electronic structure can be resolved by rotating the sample. In EMS real momentum of the bound electron is measured, not the crystal momentum and thus polycrystalline and amorphous solids are also viable targets. By using EMS to measure the the spectral functions of ordered and disordered semiconductors we attempt to establish experimentally to what extent their electronic structures differ.

2. CRYSTALLINE SILICON

The experimental spectral function of crystalline Si has been measured by the solid state EMS group at the Australian National University for experimental information see Vos et al. [6, 7]. In Fig. 1 we show the experimental spectral functions for the three high symmetry directions of single crystal Si and compared them to calculations based on full potential linear muffin tin orbital (FP-LMTO) density functional theory. Anisotropy in the electronic structures of the Si crystal result in large variations of the EMS results for different crystal directions (Fig. 1). The FP-LMTO theory matches the measured band dispersion amazingly well. Theory fails to accurately predict the relative band intensities, with, for example, theory predicting the bottom of the band to be most intense, whereas in the experiment the top of the band has the largest intensity. The clear differences between the measured and calculated spectral functions for the Si $\langle 100 \rangle$ direction can be attributed to finite experiment momentum resolution [8]. These results have been analysed in more detail by Kheifets et. al. [9] and Bowles et. al. [10]. With the validity of the method established by the good agreement between experiment and theory for single crystal samples, we are now in a good position to study the less

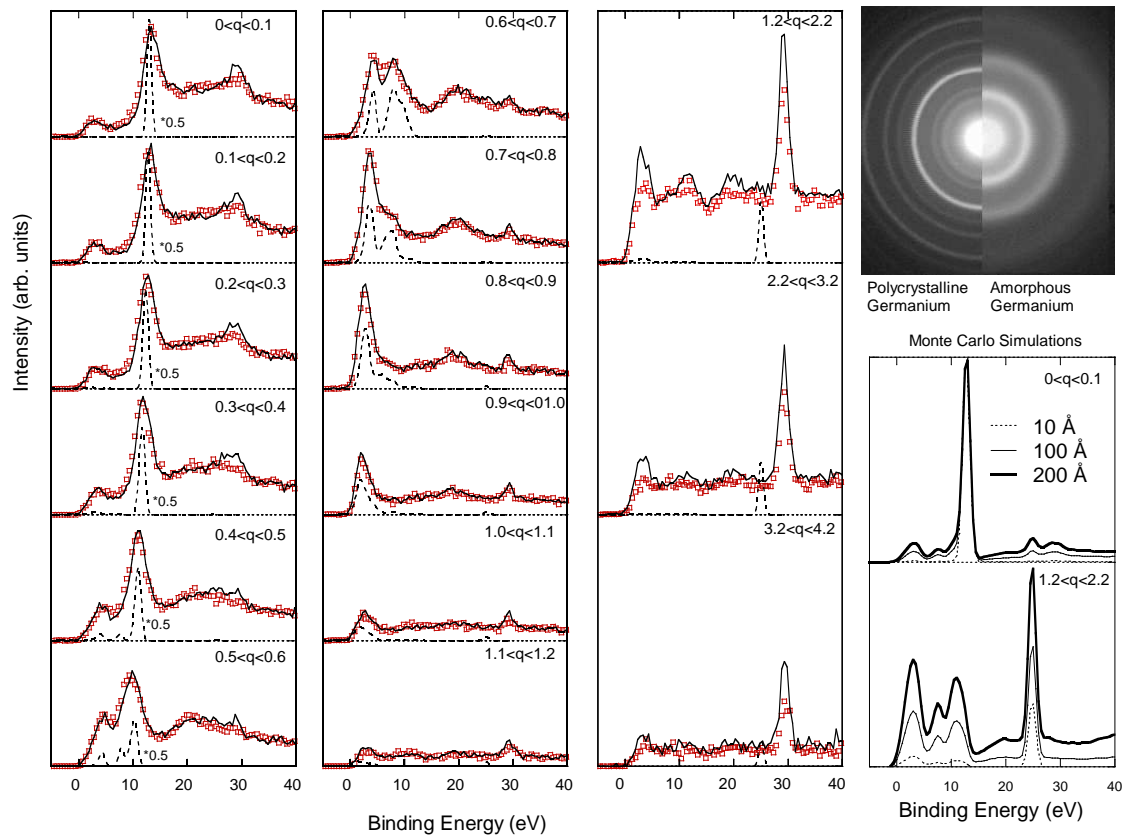


FIGURE 2. The experimental spectra of amorphous Germanium (squares), polycrystalline Germanium (full line) at momentum intervals as indicated. Also shown are calculated spectra based on the spherically averaged theory of single crystal. Intensity of theory in the left panel is divided by 2. The diffraction patterns shown at the right is measured *in situ* for the polycrystalline and amorphous film. The lower right panel shows the influence of the thickness on the 3d intensity as derived from Monte Carlo simulations.

understood amorphous form, and compare its electronic structure with the results for polycrystalline films.

3. POLYCRYSTALLINE VERSUS AMORPHOUS GERMANIUM

Amorphous semiconductor films, suitable for EMS can be made by evaporation on thin (30 Å) carbon films. Polycrystalline films can be made by annealing these films. However in the case of silicon a reaction at the Si/C interface produced silicon carbide [11]. This problem does not occur for germanium. The measured spectral function for amorphous and polycrystalline germanium as well as their electron diffraction patterns are shown in Fig. 2. The polycrystalline diffraction pattern is a 360° smearing of the single crystal diffraction pattern, resulting in sharp concentric circles. Amorphous Ge samples however with their large distribution of bond lengths and angles give much broader diffraction rings.

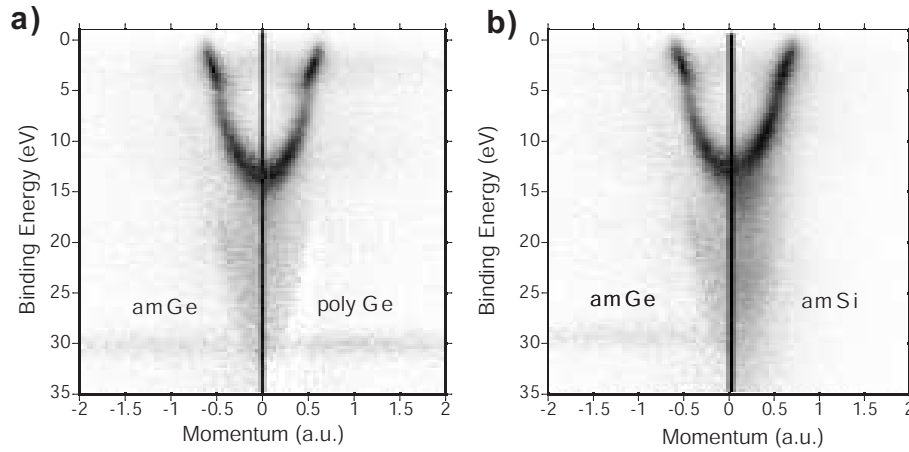


FIGURE 3. a) The measured spectral functions for disordered Ge, amorphous (left) and polycrystalline (right). (b) The measured spectral functions of amorphous Ge (left) and amorphous Si (right).

It is thus surprising that, in spite of the large differences in the electron diffraction patterns, the measured spectral function of polycrystalline and amorphous germanium are very similar indeed. The two sets of spectra were normalised using a single factor. Within the statistical limits the spectra near zero momentum are identical, with the exception that the plasmon loss peak (16 eV below the main peak) is slightly more pronounced in the polycrystalline case. This is in agreement with the findings of Zeppenfeld and Raether that the plasmon energy loss peak is more intense in electron energy loss spectra of polycrystalline samples compared to amorphous samples [12]. The second difference is in the spectrum for the 0.6-0.7 a.u. momentum range where there is a minimum in intensity near 5 eV for the polycrystalline case. In the amorphous case this minimum is less pronounced. This momentum range coincides for many crystalline orientations with the first Brillouin zone boundary, and hence we are sensitive for the splitting between the inner and outer valence band in these momentum range. In spite of the spherical averaging this splitting is still evident in the polycrystalline data. The fact that this is less evident for the amorphous case is expected, as the concept of the first Brillouin zone is not so well defined for amorphous semiconductors where the atomic bonds and angles vary by about 10% [13] relative to the crystalline case. Band gaps between the conduction band and valence band are found experimentally and in calculations for amorphous semiconductors [14, 15].

Most surprisingly the most pronounced differences are found in the high momentum spectra (above 1.2 a.u.) of Fig. 2. In the polycrystalline case the 3d electron appear systematically more intense compared to the amorphous case. The normalisation constant of the two measurements was chosen such that the valence band features had equal intensity. Normalisation of the 3d features to equal height would make the amorphous Ge valence band more intense than the polycrystalline one. The most likely cause of this phenomenon is that the variation in intensity is due to different elastic multiple scattering contributions due to different sample thicknesses. This possibility was investigated in Monte Carlo calculations, using the result of the FP-LMTO calculation as input [16], but assuming different sample thicknesses. These results are shown in Fig. 2 as well.

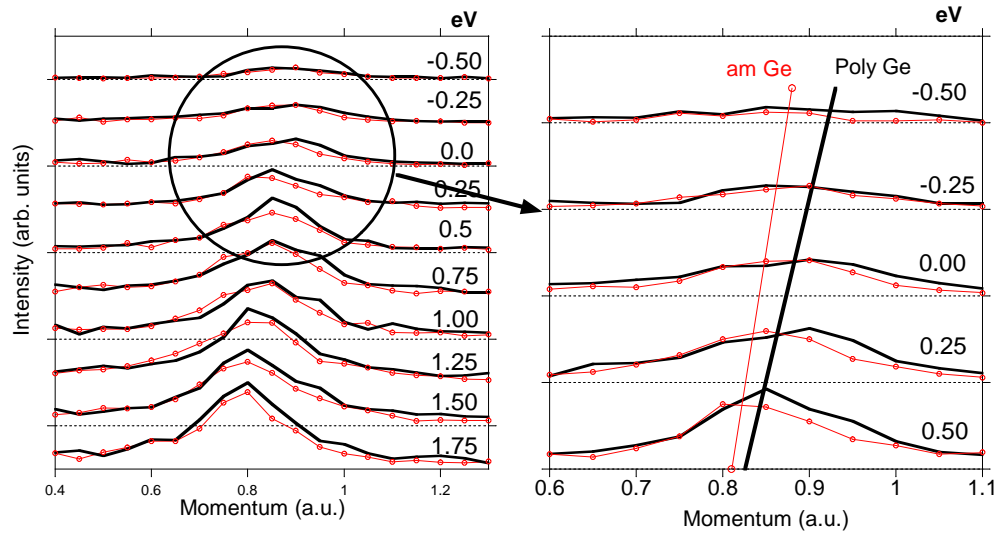


FIGURE 4. Left: Momentum profiles at different binding energies. The ‘dispersion’ appears weaker for the amorphous sample compared to the polycrystalline one. Right: a closer look at the differences in the slope of the sp-hybridised band of the amorphous and polycrystalline spectral functions.

Consider first the intensity at the bottom of the valence band. Elastic scattering will remove intensity away from zero momentum, and will cause intensity to be shifted from the peak at zero momentum to the background at the same energy, but larger momentum values. For the non-dispersing 3d feature elastic scattering will cause intensity still to contribute to the 3d peak, but now at the ‘wrong’ momentum. Hence it appears that the 3d intensity increases with thickness relative to the valence band intensity.

In Fig. 2 we show the results of the FP-LMTO calculations as well. In this calculation we treated the 3d electrons as valence electrons. In this way we obtain intensities for valence electrons and the 3d electrons in a uniform way. The calculated Ge 3d position is at somewhat smaller binding energy as the measured 3d position. Due to life time broadening (not included in the calculation) the maximum peak height near the bottom of the band is larger in the theory than in the experiment. For easy comparison we re-scaled theoretical intensity in the left panel of Fig. 2. The measured 3d intensity is significantly larger than the calculated one, another indication that elastic multiple scattering reduces the valence band intensity more than the 3d intensity.

We compare the measured spectral function of amorphous germanium as a grey-scale plot with that of polycrystalline germanium Fig.3(a) and with amorphous silicon in Fig. 3(b). Again the differences are minor. For Ge the 3d level can just be distinguished near 29.5 eV binding energy, and this feature is of course absent in Si. The silicon features are somewhat broader. The amorphous silicon spectra resemble the theoretical results of Hickey and Morgan calculations at least semi-quantitatively. [3]

Upon examining the spectral function of amorphous and polycrystalline Ge one more difference is noticeable. The slope at the top of the bands near the Fermi level is slightly different. This point is emphasised in Fig. 4. The band gap is due to a periodic potential that interacts strongly with electron states with \mathbf{k} vectors near the Brillouin zone boundary. In the amorphous case this periodic potential is less well defined due

to the lack of long range order and the dispersion for a more disordered sample would deviate less from a free electron behaviour. The polycrystalline slope near the top of the band (13.3 ± 3.6 eV/a.u.) is much smaller than the amorphous slope (20.4 ± 8.1 eV/a.u.). This electronic structure effect could be an experimental indication of the crystalline order differences of the two samples.

4. CONCLUSION

Single crystal Si spectral functions were shown in comparison to full potential linear muffin tin orbital calculations. Agreement was in general quite good. The anisotropy of the band structure is well resolved and the observed band dispersion was very well reproduced by theory. Based on this understanding of single crystal silicon result we want to compare the electronic structure of amorphous silicon and amorphous and polycrystalline germanium. For momenta near the edge of the first Brillouin zone the spectra are split in a lower and upper band contribution for polycrystalline Ge but somewhat less for amorphous Ge and Si. This can be attributed to the lack of long range order in the latter cases. A noticeable difference in the Ge 3d level to valence band intensity ratio between amorphous and polycrystalline Ge and amorphous Ge was found but is not understood. The position of the maxima in the Ge momentum profiles near the top of the band are more dependent on their binding energy than the amorphous ones. Besides these minor differences we find a surprisingly large similarity between the amorphous and polycrystalline Ge spectra.

This research was made possible by a research grant from the Australian Research Council.

REFERENCES

1. W. Zachariasen, *J. Am. Chem. Soc.*, **54**, 3841–3851 (1932).
2. S. Bose, K. Winer, and O. Andersen, *Phys. Rev. B*, **37**, 6262–6277 (1988).
3. B. Hickey, and G. Morgan, *J. Phys. C: Solid State Phys.*, **19**, 6195–6209 (1986).
4. I. McCarthy, and E. Weigold, *Rep. Prog. Phys.*, **54**, 789–879 (1991).
5. E. Weigold, and I. McCarthy, *Electron momentum spectroscopy*, Physics of Atoms and Molecules, Kluwer Academic, 1999.
6. M. Vos, G. Cornish, and E. Weigold, *Rev. Sci. Instrum.*, **71**, 3831–3840 (2000).
7. M. Vos, and E. Weigold, *J. Elec. Spec. Rel. Phenom.*, **112**, 93–106 (2000).
8. M. Vos, V. Sashin, C. Bowles, A. Kheifets, and E. Weigold, *J. Phys. Chem. of Sol.*, **65**, 2035–2039 (2004).
9. A. Kheifets, V. Sashin, M. Vos, E. Weigold, and F. Aryasetiawan, *Phys. Rev. B*, **68**, Art. No. 233205 (2003).
10. C. Bowles, A. Kheifets, V. Sashin, M. Vos, and E. Weigold, *J. Elec. Spec. Rel. Phen.*, **141**, 95–104 (2004).
11. Y. Q. Cai, M. Vos, P. Storer, A. S. Kheifets, I. E. McCarthy, and E. Weigold, *Solid State Communications*, **95**, 25–29 (1995).
12. K. Zeppenfeld, and H. Raether, *Zeitschrift für Physik*, **193**, 471 (1966).
13. S. Moss, and J. Gracyk, *Phys. Rev. Lett.*, **23**, 1167 (1969).
14. D. Weaire, *Phys. Rev. Lett.*, **26**, 1541–1543 (1971).
15. D. Weaire, and F. Thorpe, *Phys. Rev. B*, **4**, 2508–2520 (1971).
16. M. Vos, and M. Bottema, *Physical Review B*, **54**, 5946–5954 (1996).